European Journal of Cancer 118 (2019) 70–81

Available online at www.sciencedirect.com

ScienceDirect

journal homepage: www.ejcancer.com

Original Research

Identification of a functional polymorphism within the 3′-untranslated region of denticleless E3 ubiquitin protein ligase homolog associated with survival in acral melanoma

Lu Yang [a,1], Jie Dai [a,1], Meng Ma [a,b], Lili Mao [a], Lu Si [a], Chuanliang Cui [a], Xinan Sheng [a], Zhihong Chi [a], Sifan Yu [a], Tianxiao Xu [a], Jinyu Yu [a], Yan Kong [a,**], Jun Guo [a,*]

[a] *Key Laboratory of Carcinogenesis and Translational Research (Ministry of Education/Beijing), Department of Renal Cancer and Melanoma, Peking University Cancer Hospital and Institute, Beijing, 100142, China*
[b] *Department of Radiotherapy, Beijing Chest Hospital, Capital Medical University, Beijing Tuberculosis and Thoracic Tumor Research Institute, Beijing, 101149, China*

Received 28 November 2018; received in revised form 7 May 2019; accepted 20 June 2019
Available online 17 July 2019

KEYWORDS
Acral melanoma;
DTL;
Genetic variants;
hsa-miR-4672;
Prognosis

Abstract ***Background:*** High expression of denticleless E3 ubiquitin protein ligase homologue (DTL) correlates with poor disease-free survival and overall survival in cutaneous melanoma, but the molecular features and clinical significance of this gene in acral melanoma (AM) remain unclear.

Methods: The expression levels of DTL were compared between AM and benign melanocytic nevi using existing Gene Expression Omnibus data and validated in fresh frozen tissues. Two candidate tag single-nucleotide polymorphisms (SNPs) in the 3′-untranslated region (3′UTR) of *DTL* in patients with AM were sequenced and analysed for their association with survival in a discovery cohort (n = 570), and the significant SNP was subjected to a replication cohort (n = 201). The expression of DTL was evaluated by immunohistochemistry. The microRNA interacting with rs11275300:C > G was predicted using *in silico* target prediction tools and validated by *in vitro* analysis.

Results: DTL was overexpressed in AM compared with benign melanocytic nevi.

* *Corresponding author*: Department of Renal Cancer and Melanoma, Peking University Cancer Hospital & Institute, 52# Fucheng Road, Haidian District, Beijing, 100142, China.
** *Corresponding author*: Department of Renal Cancer and Melanoma, Peking University Cancer Hospital & Institute, 52# Fucheng Road, Haidian District, Beijing, 100142, China.
E-mail addresses: k-yan08@163.com (Y. Kong), guoj307@126.com (J. Guo).
[1] L. Yang and J. Dai contributed equally to this work.

https://doi.org/10.1016/j.ejca.2019.06.006

rs11275300:C > G was found to be significantly associated with progression-free survival and overall survival of patients with AM in both cohorts and the combined cohort. Furthermore, the DTL expression level in the patients with the rs11275300:G allele was higher than that in patients with the CC genotype. *In vitro* analysis demonstrated that *DTL* was a direct target of hsa-miR-4672, and the rs11275300:G allele interfered with the binding affinity of hsa-miR-4672 with the 3′UTR of *DTL* and thereby increased *DTL* expression.

Conclusion: The rs11275300:G allele in the 3′UTR of *DTL* may lead to a poor prognosis and allele-specific increase in the expression of *DTL* by post-transcriptional regulation in AM.

1. Introduction

The incidence of melanoma is rapidly increasing globally, and malignant melanoma is the major cause of death from skin cancer. Melanoma can be subdivided into four subtypes based on clinical and histological features: acral melanoma (AM), mucosal melanoma, cutaneous melanoma with chronic sun-induced damage (CSD) and cutaneous melanoma without such damage (non-CSD) [1]. AM is rare in Caucasians (1–7%) [2]; however, dark-skinned populations are more prone to develop AM, with a prevalence of about 41–70% [3–5]. Meanwhile, AM accounts for nearly 50% of all melanomas in China [4]. The genetic alteration spectrum of AM differs greatly from that of non-acral cutaneous melanoma (CM), as the mutation burden of AM is significantly lower than that of CM, but somatic structural variants are more frequent in AM than in CM [6]. *BRAF* (~50%) and *NRAS* (25–30%) are the most important mutations in CM [7], whereas the mutation frequencies of *BRAF*, *NRAS* and *CKIT* in Chinese AM are 15.5%, 8.8% and 11.9%, respectively [1,8,9]. Therefore, uncovering other potential prognostic predictive factors will help to clarify AM pathogenesis and develop novel therapeutic approaches for AM.

Denticleless E3 ubiquitin protein ligase homologue (DTL) is also known as DNA replication factor 2, regulating the expression of various cell cycle regulatory proteins and maintaining the integrity of DNA replication and repair [10]. The expression level of DTL has been reported to be elevated in multiple human malignancies, such as breast cancer and ovarian cancer [11–13]. DTL was also found to be overexpressed in 59% primary hepatocellular carcinomas and correlated with the advanced tumour stage and poor patient survival [10]. Moreover, its potential as a prognostic biomarker in Ewing sarcoma and gastric cancer has been demonstrated [11,14]. According to the mRNA expression data of the Talantov melanoma data set, *DTL* is remarkably overexpressed in CM compared with benign melanocytic skin nevi [15]. Furthermore, data from The Cancer Genome Atlas database revealed that patients with melanoma with higher *DTL* expression exhibit shorter disease-free survival (DFS) and overall survival (OS) [16]. However, most of these data are from Caucasians with non-acral CM; the molecular characterisation and prognostic value of *DTL* in AM remain unknown.

Increasing evidence strongly implicates the crucial role of the 3′-untranslated region (3′UTR) in the post-transcriptional regulation of gene expression, including translation efficiency, nuclear export, subcellular targeting and mRNA stability [17,18]. MicroRNAs (miRNAs) mediate mRNA degradation and translational repression by base pairing with the 3′UTR of target mRNAs [19]. Genetic variants in miRNA-binding sites have been identified to be associated with human disorders ranging from Parkinson disease to cancer [20,21]. Single-nucleotide polymorphisms (SNPs) are the most frequent form of sequence variations in the human genome, and SNPs in 3′UTR sites have been identified as promising genetic factors that may disrupt or create seed pairing regions in the miRNA, thereby altering gene expression and influencing the susceptibility to tumorigenesis [22,23].

In this study, we detected the expression of DTL in AM, screened the 3′UTR polymorphisms of *DTL* in two independent AM cohorts, investigated the association of tag SNP genotypes with the survival and clinical characteristics of patients with AM, and recognised a promising candidate molecular indicator with potential prognostic value. Furthermore, we validated the hypothesis that a functional polymorphism in the 3′UTR site of *DTL* might affect the post-transcriptional regulation of hsa-miR-4672 and influence *DTL* expression.

2. Materials and methods

2.1. Study design and patients

This retrospective exploratory study was approved by the Ethics Committee of Beijing Cancer Hospital & Institute and conducted in adherence to the principles of the Declaration of Helsinki. Signed informed consent for the purpose and procedures of this study was

obtained from each patient with AM. A total of 771 patients with AM who were hospitalised at Peking Cancer Hospital and Institute from January 2007 to January 2017 were enrolled in the discovery cohort (n = 570) or replication cohort (n = 201) based on the following criteria: availability of formalin-fixed paraffin-embedded (FFPE) or fresh frozen samples; patients who received standard treatment and availability of detailed clinical and pathological data, including age, sex, tumour-node-metastasis stage, Breslow thickness, ulceration state, plasma lactate dehydrogenase (LDH) levels. Patients treated with BRAF inhibitors or immunotherapies were not included in the study. A group of 216 patients with non-acral CM were enrolled in an independent cohort accordingly. The last follow-up was carried out in August 2018; the median follow-up time of the discovery and replication cohorts was 35.8 months (range, 0.2–159.3 months) and 39.7 months (range, 2.9–109.9 months), respectively. The time period between disease confirmation and progression (relapse and metastasis) or disease-related death was determined as progression-free survival (PFS). OS was calculated from the date of disease confirmation to the date of last follow-up or death.

2.2. Cell culture

HEK293T and A875 cell lines were purchased from the Cell Bank of the Chinese Academy of Sciences and maintained in Dulbecco's modified eagle's medium (DMEM) with 10% foetal bovine serum supplemented with 100 U/mL penicillin, 100 mg/mL streptomycin and 2 mM GlutaMAX in a humidified incubator with 5% CO_2 at 37 °C. All cell culture reagents were purchased from Gibco.

2.3. Gene expression analysis of chip data sets for AM

We used 'acral melanoma' as a keyword to retrieve gene expression data in the Gene Expression Omnibus (GEO) database. We extracted a gene expression data set including nevi, primary AM and primary CM samples (GSE46517) and two data sets including AM and CM samples (GSE80435 and GSE22155). The raw cool edit loop (CEL) data were downloaded; probe and genetic information was connected using the annotation information of chips and the raw data were normalised using the RMA method from the Bioconductor and R software packages. The gene expression profiles of six primary and 12 lymph node metastatic AM samples were analysed using the GeneChip PrimeView Human Gene Expression Array (Affymetrix), as previously reported [24].

2.4. SNP selection and genotyping

Candidate SNPs of *DTL* were selected based on the public databases dbSNP, TogoVar (the national bioscience database center (NBDC) integrated database of the Japanese genomic variation) and PanSNPdb (a Pan-Asian SNP database) according to the following criteria: (i) minor allele frequencies (MAFs) ≥ 0.05 in the East Asian population; (ii) tag SNPs from dbSNP in the Asian population with $r^2 > 0.8$ (https://snpinfo.niehs.nih.gov/snpinfo/snaptag.html); (iii) potential functional SNPs in the 5′UTR, missense variants in exons and variants in miRNA-binding sites of the 3′UTR.

Genomic DNA was extracted using the Universal Genomic DNA Kit (CWBIO). Polymerase chain reaction (PCR) amplification and Sanger sequencing were performed to determine the tag SNP genotypes of *DTL*. Chromatography results were analysed by BLAST, and the tag SNP genotypes were determined by manual review. In patients with whole-blood leucocyte samples available, the genotypes were verified by the same method. Fifty samples were randomly selected for replicated detection and analysis by a different investigator.

2.5. RNA extraction and qRT-PCR

Total RNAs from fresh frozen AM tissues, benign melanocytic skin nevi, and cell lines were extracted using mirVanaTM miRNA isolation kits (Invitrogen). One microgram of total RNA was reverse transcribed into complementary DNA (cDNA) with the ReverTra Ace qPCR RT kit (Toyobo). qPCR was performed with Promega's GoTaq® qPCR Master Mix using the ABI 7500 FAST Real-Time PCR System (Applied Biosystems). The expression level of *DTL* was normalised to *GAPDH* expression. Cycle threshold (Ct) values were recorded, and the relative quantitative levels of gene expression were calculated by the $2^{-\Delta\Delta Ct}$ method.

miRNAs were reverse transcribed into cDNA with the TaqMan MicroRNA Reverse Transcription kit (Applied Biosystems). Quantitative real-time PCR (qRT-PCR) was performed with the TaqMan Universal PCR Master Mix II (Applied Biosystems). The hsa-miR-4672 and internal control gene *RNU6B* primers were purchased from Ambion.

2.6. Immunohistochemistry staining

FFPE slides were deparaffinized, and endogenous peroxidase activity was blocked with 3% H_2O_2 for 30 min in the dark. Antigen retrieval was performed in 1 mM ethylene diamine tetra-acetic acid buffer (pH 8.0) in a pressure cooker. The primary antibody against DTL (Bethyl) was diluted at 1:250, and the horseradish peroxidase (HRP)-conjugated polyclonal rabbit antibody (dilution 1:400; Dako) was used as the secondary antibody. Specific immunostaining was visualised with the chromogen aminoethyl carbazole (ZSGB BIO) and counterstaining with haematoxylin. The immunohistochemistry (IHC) score for each sample was scored as

0–3, according to the staining intensity and density, by three pathologists blinded to the genotypes of the samples.

2.7. Luciferase reporter assay

Full-length fragments of the 3′UTR sequence containing either the G or C allele of rs11275300 were amplified by PCR, and the fragments were inserted into SV40 promoter-luciferase–containing plasmids (Promega). Then, the recombinant constructs were verified by sequencing. HEK293T cells were transiently transfected with 500-ng luciferase reporter constructs and 5 pmol miRNA by Lipofectamine 3000 (Invitrogen) in 24-well plates at a density of 5×10^4 cells per well. The cells were lysed 48 h after transfection, and luciferase activity was determined using the dual-luciferase reporter system E2920 (Promega).

2.8. Oligonucleotide transfection

A875 cells were seeded into 6-well plates at a density of 3×10^5 cells per well and cultured overnight as described previously. Next, miR-4672 mimics, hairpin inhibitors or their scrambled controls (RiboBio) were transfected into cells at a concentration of 50 nM using Lipofectamine 3000. The cells were harvested after 48 h of transfection for subsequent analyses.

2.9. Western blotting

The A875 cells were lysed using radio immunoprecipitation assay (RIPA) lysis buffer (Beyotime Biotechnology) supplemented with protease inhibitors (Roche Diagnostics). The proteins were quantified using BCA assays (Thermo Scientific), and 30 μg of each protein was subjected to 10% sodium dodecyl sulfate – polyacrylamide gel electrophoresis (SDS-PAGE) and transferred onto polyvinylidene fluoride (PVDF) membranes (Roche Diagnostics). Immunodetection was performed with rabbit anti-DTL polyclonal antibody (1:5000; Bethyl Laboratories) and mouse anti-GAPDH antibody (1:5000; Abcam). Peroxidase-labelled anti–mouse or anti–rabbit IgG antibodies (1:3000; CST) were used as secondary antibodies. Immunodetection was performed using the Amersham ECL Select Western Blotting Detection Reagent (GE Healthcare). Protein band intensities were quantified using ImageJ64.

2.10. Statistical analysis

All statistical analyses were carried out using SPSS 21.0 software. Mean ± standard deviation values were used to describe normally distributed continuous data, such as age and Breslow thickness. Frequencies and percentages were used to describe categorical data. Genotype frequencies and clinical parameters such as sex, ulceration and stage were compared using the chi-square test. Breslow thickness and H-scores of the DTL protein were evaluated by two independent sample *t*-tests or the Mann–Whitney *U* test. Survival curves were established using the Kaplan–Meier method, and the results were evaluated using the log-rank test. Multivariate analysis was carried out using the Cox proportional hazard regression model. The deviations of the allele and genotype frequencies were estimated using the Hardy–Weinberg equilibrium. All statistical tests were two-sided, and significance was assigned at $P < 0.05$. The Bonferroni correction was applied in the discovery cohort according to the number of tag SNPs evaluated (threshold = 0.05/number of tag SNPs selected).

3. Results

3.1. DTL is overexpressed in AM compared with benign melanocytic skin nevi

Three gene expression data sets were extracted from the GEO database, including nine nevi, 12 primary AM, and 60 primary CM samples. The results showed that the expression levels of DTL in both AM and CM were significantly higher compared with benign melanocytic skin nevi, whereas there was no difference between AM and CM (Fig. 1A), and the tendency was consistent in

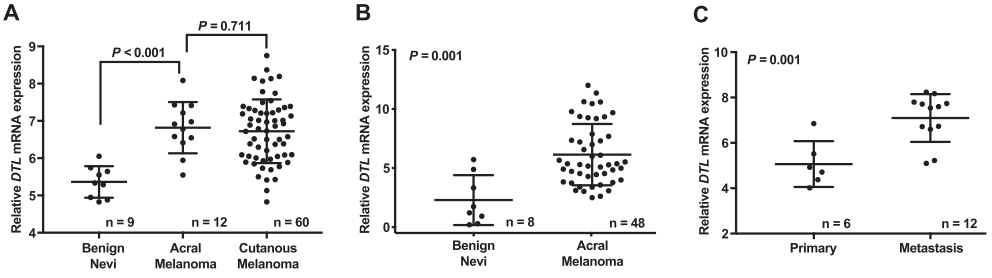

Fig. 1. ***DTL* is overexpressed in AM compared with benign nevi**. (A) *DTL* mRNA expression is higher in primary AM and CM than in benign nevi (GSE46517, GSE80435 and GSE22155). The *DTL* expression levels were normalised using the RMA method (B) *DTL* mRNA expression is higher in AM than in benign nevi. The *DTL* mRNA levels were measured by qRT-PCR and expressed on a $\log_2$ scale (C) *DTL* mRNA expression was high in metastatic AM tissues. The *DTL* expression levels were normalised using the RMA method. AM, acral melanoma; CM, cutaneous melanoma; PCR, polymerase chain reaction.

Table 1
Cox regression analysis of risk factors associated with PFS.

Clinical character	Group	Discovery				Replication			
		Univariate HR (95% CI)	*P* value	Multivariate HR (95% CI)	*P* value	Univariate HR (95% CI)	*P* value	Multivariate HR (95% CI)	*P* value
Age	≥60 vs. <60	0.918 (0.742–1.136)	0.433			1.258 (0.860–1.843)	0.237		
Sex	Female vs. male	1.105 (0.904–1.351)	0.330			1.072 (0.775–1.484)	0.673		
Ulceration	Yes vs. no	1.201 (0.956–1.508)	0.116			1.370 (0.988–1.900)	0.059		
TNM stages	III and IV vs. I and II	2.252 (1.823–2.783)	<0.001*	2.138 (1.721–2.655)	<0.001*	3.371 (2.329–4.880)	<0.001*	3.253 (2.240–4.722)	<0.001*
Thickness	≥4 mm vs. <4 mm	1.271 (0.994–1.711)	0.114			1.346 (0.819–2.214)	0.241		
LDH level	Elevated vs. normal	2.334 (1.781–3.059)	<0.001*	1.837 (1.392–2.425)	<0.001*	1.126 (0.551–2.299)	0.745		
rs111275300	GC + GG vs. CC	1.598 (1.297–1.967)	<0.001*[a]	1.629 (1.321–2.009)	<0.001*	1.682 (1.179–2.399)	0.004*	1.453 (1.015–2.082)	0.041*
rs1387815	TG + GG vs. TT	0.919 (0.744–1.135)	0.434						
BRAF	Mut vs. WT	1.306 (1.030–1.657)	0.028*	1.230 (0.969–1.362)	0.089	0.971 (0.677–1.392)	0.871		

*, $P < 0.05$.
LDH, lactate dehydrogenase; PFS, progression-free survival; CI, confidence interval; HR, hazard ratio; WT, wild type; Mut, mutation; TNM, tumour-node-metastasis.
[a] *P* values significant after adjusted for multiple comparisons with the Bonferroni correction $P < 0.025$ for significance.

the three independent data sets (Fig. A1). To verify the aforementioned conclusion from GEO, we analysed the DTL expression levels in eight benign melanocytic skin nevi from the palm or foot and 48 AM samples by qRT-PCR. The result was consistent with GEO data sets in that the expression of DTL in AM was much higher than that in benign nevi (Fig. 1B). Furthermore, according to our previous study of the gene expression profiles of six primary and 12 lymph node metastatic AM samples by tissue microarray analysis [24], the DTL expression level was even higher in the metastatic sites of AM compared with the primary lesions (Fig. 1C). All these data demonstrated the same results as those in CM. DTL was also overexpressed in AM, and the

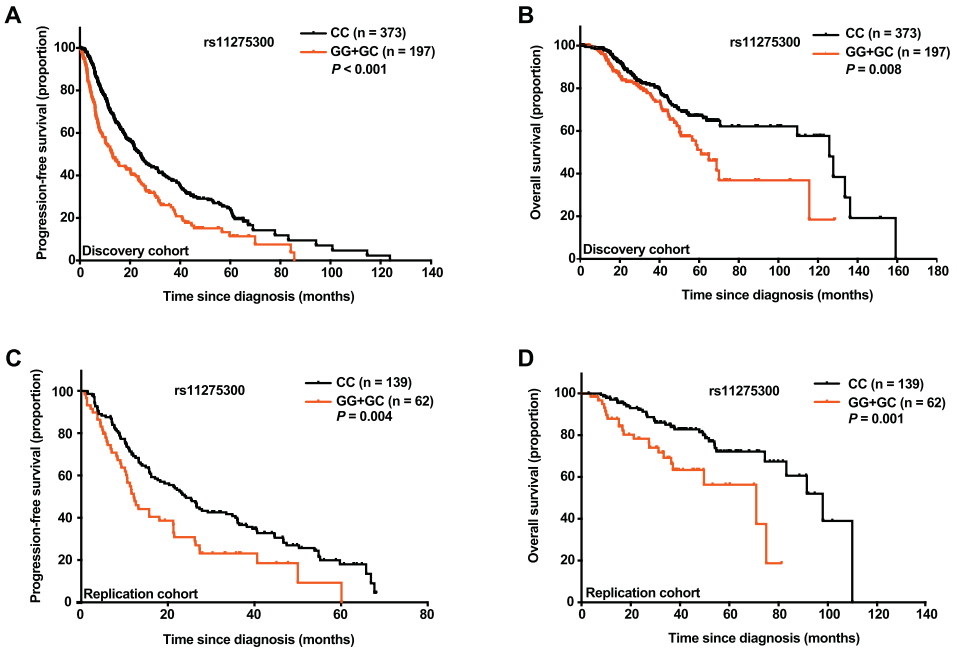

Fig. 2. **The *DTL* rs11275300 genotype is correlated with prognosis in AM**. Kaplan–Meier curves of PFS (A) and OS (B) according to the rs11275300 genotype in the discovery cohort. Kaplan–Meier curves of PFS (C) and OS (D) according to the rs11275300 genotype in the replication cohort. AM, acral melanoma; PFS, progression-free survival; OS, overall survival.

expression level was associated with the malignant degree.

3.2. Association of tag SNPs of DTL with survival in patients with AM

As DTL was overexpressed in AM compared with benign melanocytic nevi, we hypothesised that the polymorphisms of DTL might be associated with DTL expression and survival of patients with AM. Two candidate tag SNPs were selected, including rs1387815 and rs11275300, both of which are located in the 3′UTR of DTL (Fig. A2). According to the discovery cohort, the MAFs of rs1387815 and rs11275300 were 0.200 and 0.201, respectively, and the genotype distribution of both two tag SNPs in our cohorts showed no departure from the Hardy–Weinberg equilibrium (Table A1).

The clinical significance of these two tag SNPs was analysed in the discovery cohort including 570 patients with AM. No significant difference in PFS (hazard ratio [HR]: 0.919, 95% confidence interval [CI]: 0.744–1.135, $P = 0.434$) or OS (HR: 1.028, 95% CI: 0.729–1.488, $P = 0.875$) between patients with the rs1387815:G allele and those with the TT genotype was observed (Table 1, Fig. A3) in the discovery cohort. For rs11275300, patients with the rs11275300:G allele had a median PFS of 13.1 months (95% CI: 9.5–16.8 months), whereas patients with the CC genotype had a median PFS of 24.3 months (95% CI: 20.9–27.7 months), and univariate Cox analysis and Kaplan–Meier survival analysis showed that patients with the rs11275300:G allele had shorter PFS than patients with the CC genotype (HR: 1.598, 95% CI: 1.297–1.967, $P < 0.001$; Fig. 2A). In addition, the median OS values of patients with the rs11275300:G allele and CC genotype were 61.1 months (95% CI: 50.9–71.3 months) and 125.7 months (95% CI: 107.0–144.4 months), respectively, demonstrating that OS of patients with the rs11275300:G allele was shorter than that of patients with the CC genotype (HR: 1.572, 95% CI: 1.120–2.206, $P = 0.009$; Fig. 2B). After the Bonferroni correction ($P < 0.025$), rs11275300 remained significantly associated with PFS and OS of AM. Multivariate Cox regression analysis was performed to further adjust for any residual confounding effect on PFS and OS, and the results revealed the rs11275300:G allele to be significantly associated with a shorter PFS (HR: 1.629, 95% CI: 1.321–2.009, $P < 0.001$) and OS (HR: 1.435, 95% CI: 1.016–2.028, $P = 0.040$) in the discovery cohort.

In the replication cohort, the associations of the rs11275300 genotype with PFS (Table 1, Fig. 2C) and OS (Table 2, Fig. 2D) were consistent in the discovery cohort according to univariate and multivariate analyses. Furthermore, the prognostic effects of the rs11275300 genotype remained significant in the

Table 2
Cox regression analysis of risk factors associated with OS.

Clinical character	Group	Discovery				Replication			
		Univariate HR (95% CI)	*P* value	Multivariate HR (95% CI)	*P* value	Univariate HR (95% CI)	*P* value	Multivariate HR (95% CI)	*P* value
Age	≥60 vs. <60	0.912 (0.638–1.303)	0.612			1.096 (0.583–2.060)	0.776		
Sex	Female vs. male	1.360 (0.974–1.899)	0.071			0.732 (0.422–1.270)	0.267		
Ulceration	Yes vs. no	1.586 (1.035–2.429)	0.034*	1.396 (0.909–2.144)	0.127	4.430 (2.283–8.598)	<0.001*	4.199 (2.135–8.259)	<0.001*
TNM stages	III and IV vs. I and II	2.903 (1.992–4.229)	<0.001*	2.519 (1.178–3.693)	<0.001*	3.542 (1.774–7.705)	<0.001*	3.401 (1.696–6.818)	0.001*
Thickness	≥4 mm vs. <4 mm	1.356 (0.822–2.237)	0.234			1.567 (0.555–4.426)	0.396		
LDH level	Elevated vs. normal	3.436 (2.369–4.984)	<0.001*	2.519 (1.708–3.713)	<0.001*	4.878 (2.152–11.059)	<0.001*	3.523 (1.539–8.065)	0.003*
rs111275300	GC + GG vs. CC	1.572 (1.120–2.206)	0.009*[a]	1.435 (1.016–2.028)	0.040*	2.476 (1.394–4.398)	0.002*	2.012 (1.119–3.616)	0.019*
rs1387815	TG + GG vs. TT	1.028 (0.729–1.448)	0.875						
BRAF	Mut vs. WT	0.897 (0.588–1.368)	0.613			1.149 (0.619–2.133)	0.661		

*, $P < 0.05$.
CI, confidence interval; OS, overall survival; HR, hazard ratio; WT, wild type; Mut, mutation; TNM, tumour-node-metastasis.
[a] *P* values significant after adjusted for multiple comparisons with the Bonferroni correction $P < 0.025$ for significance.

combined cohort (Table A2–3, Fig. A4A and B). We divided the patients into three groups according to the genotype or rs11275300, and the results showed that it was still associated with PFS and OS (Fig. A5). We further analysed the association of rs11275300:C > G with CM in a cohort of 216 Chinese patients with non-acral CM, and the basic characteristics of the CM cohort are listed in Table A4. The MAF of rs11275300:C > G in the Chinese CM cohort was 0.199, which was similar to the MAF in patients with AM (Table A5). However, no association was observed between the rs11275300 genotype with PFS (HR: 1.035, 95% CI: 0.737–1.453, $P = 0.843$) or OS (HR: 0.972, 95% CI: 0.571–1.652, $P = 0.915$) of patients with non-acral CM (Fig. A4C and A4D). These results indicated that the association of the rs11275300:G allele with shorter survival was specific in patients with AM.

3.3. Correlation of the rs11275300 genotype to the clinical characteristics in patients with AM

Patient characteristics and association of the rs11275300 genotypes with these characteristics are summarised in Table 3. We identified that the rs11275300 genotype was significantly associated with the LDH level in the discovery cohort as the patients with the rs11275300:G allele were more likely to have a higher LDH level than patients with the CC genotype (19.3% vs. 9.7%, $P = 0.002$). No significant association with LDH was confirmed in the replication cohort as only 13 patients had elevated LDH levels (8.1% vs. 5.8%, $P = 0.539$). We also analysed the association of the rs11275300 genotype with the clinical characteristics of AM by combining the discovery and replication cohorts into one combined cohort, and the results were similar with the discovery cohort: the rs11275300:G allele was associated with high LDH expression (16.6% vs. 8.6%, $P = 0.002$; Table A6). No other characteristics were found to be correlated with the rs11275300 genotype.

3.4. Correlation of the rs11275300 genotype with DTL protein expression in AM

FFPE slides of 148 patients with AM were subjected to IHC staining for analysing DTL expression. Among the 103 patients with the CC genotype, the positive detection rate for DTL was 72.8% (75/103), which was significantly different from that of patients with the rs11275300:G allele (88.9%, 40/45; $P = 0.033$). IHC staining was scored from 0 to 3 (Fig. 3A), and the results showed that the DTL expression level in patients with the rs11275300:G allele was significantly higher than that in patients with the CC genotype ($P = 0.007$; Fig. 3B). These data indicated that the rs11275300:G

Table 3
Correlation of *DTL* rs11275300 genotype to clinical characteristics of AM.

Clinical character	Discovery				Replication			
	No.	rs11275300 genotype			No.	rs11275300 genotype		
		CC	GC + GG	*P* value[a]		CC	GC + GG	*P* value[a]
Age (years)				0.46				0.822
Median (range)		53.35 ± 13.92	52.49 ± 13.31			48.30 ± 14.41	48.79 ± 13.59	
Sex n (%)				0.291				0.761
Male	284	192 (51.5)	92 (46.7)		103	70 (50.4)	33 (53.2)	
Female	286	181 (48.5)	105 (53.3)		98	69 (49.6)	29 (46.8)	
Ulceration n (%)				0.636				0.358
Yes	392	259 (69.4)	133 (67.5)		109	72 (51.8)	37 (59.7)	
No	178	114 (30.6)	64 (32.5)		92	67 (48.2)	25 (40.3)	
Thickness (mm)				0.823				0.237
Median (range)		4.62 ± 3.25	5.13 ± 4.30			3.87 ± 2.35	4.57 ± 3.43	
BRAF n (%)				0.930				0.844
WT	456	298 (79.9)	158 (80.2)		144	99 (71.2)	45 (72.6)	
Mut	114	75 (20.1)	39 (19.8)		57	40 (28.8)	17 (27.4)	
LDH level[b] n (%)				0.002*				0.539
Elevated	74	36 (9.7)	38 (19.3)		13	8 (5.8)	5 (8.1)	
Normal	496	337 (90.3)	159 (80.7)		188	131 (94.2)	57 (91.9)	
Stages n (%)				0.344				0.172
I	28	19 (5.1)	9 (4.6)		11	9 (6.5)	2 (3.2)	
II	226	144 (38.6)	82 (41.6)		66	51 (36.7)	15 (24.2)	
III	236	163 (43.7)	73 (37.1)		100	65 (46.8)	35 (56.5)	
IV	80	47 (12.6)	33 (16.8)		24	14 (10.1)	10 (16.1)	

*, $P < 0.05$.
AM, acral melanoma; LDH, lactate dehydrogenase; Mut, mutation; WT, wild type.
[a] For evaluation of age, the two independent sample t-tests was used. For evaluation of sex, ulceration and stages, the chi-square tests were used. For evaluation of thickness, two independent sample *t*-tests or Mann–Whitney *U* tests were used.
[b] The plasma LDH level of each patient was recorded and graded as follows: LDH level of 109–245 IU/L graded as normal and LDH level >245 IU/L graded as elevated.

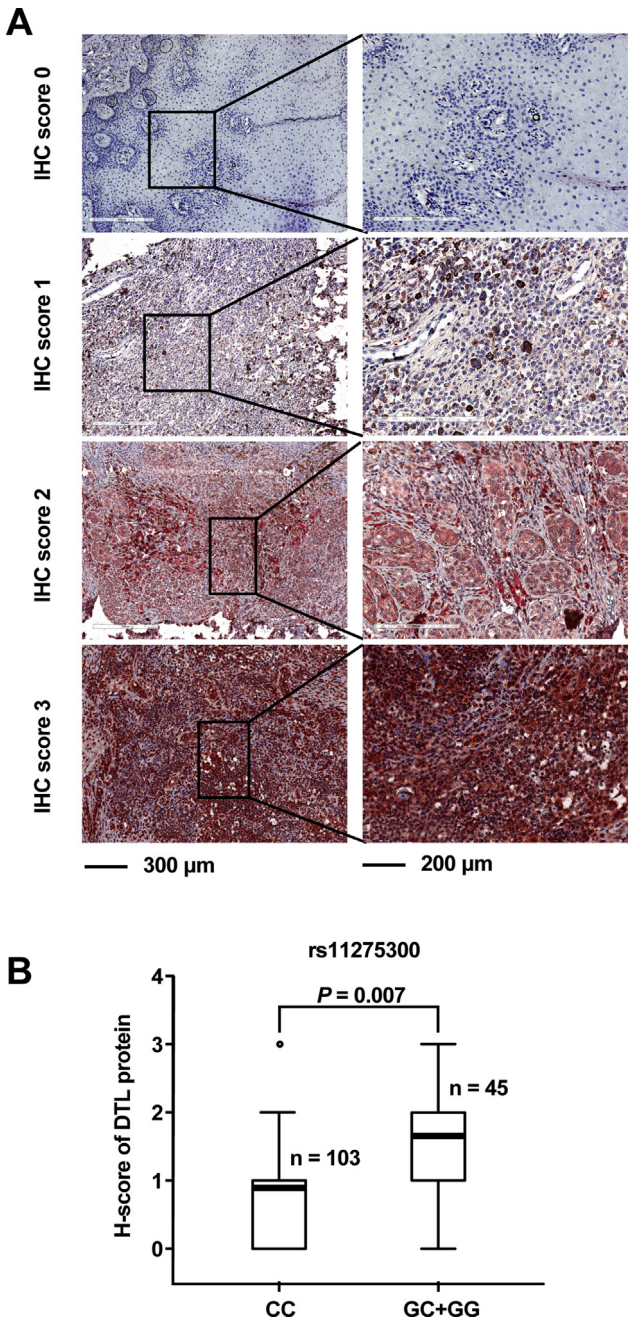

Fig. 3. **The *DTL* rs11275300 genotype is correlated with the DTL protein expression level in AM**. (A) Representative IHC staining images of DTL in FFPE specimens of AM. Red staining of the cytoplasm and nucleus was considered positive. Black/brown granules indicate melanin pigments. The staining intensity for each sample was scored as 0 (no tumour cell staining), 1 (weak), 2 (moderate) and 3 (strong) by pathologists blinded to the genotype of the samples (B) Correlation between DTL expression and the rs11275300 genotype. Significance was assessed by the Mann–Whitney *U* test. DTL, denticleless E3 ubiquitin protein ligase homologue; IHC, immunohistochemistry; AM, acral melanoma; FFPE, formalin-fixed paraffin-embedded.

allele might lead to increased expression of the DTL protein.

3.5. Search for variants in linkage disequilibrium with rs11275300

Other variants in linkage disequilibrium (LD) with rs11275300:C > G might affect *DTL* expression by regulating pre-mRNA splicing, promoter activity or mRNA stability; therefore, we tested this using the 1000 Genomes Project Phase 3 data (https://phase3browser.1000genomes.org/index.html). However, no variants were found to be in LD with rs11275300:C > G when the threshold was set as $r^2 \geq 0.05$ in all populations.

3.6. Predicted miRNAs that potentially target DTL rs11275300

Candidate miRNAs that could interact with the 3′UTR sequences of *DTL* containing rs11275300 were predicted using mirSNP, TargetScan, miRBase and PolymiRTS Database version 3.0 [25–28]. Three miRNAs were discovered, including hsa-miR-4672, hsa-miR-1910-5p and hsa-miR-6768-5p (Fig. 4A). RNAhybrid [29] was used to predict the minimum free energy (MFE) for hybridisation of the three miRNAs to *DTL* 3′UTR sequences containing rs11275300:C > G, and the results showed that the MFE values of the rs11275300:G allele were higher than those of the rs11275300:C allele for hybridisation with all three miRNAs (Table A7), which means that the affinity to these miRNAs reduced in the rs11275300:G allele.

Dual-luciferase reporter assays were performed to validate allele-specific effects of rs11275300 on *DTL* expression in the presence of predicted miRNAs. Detailed sequences of plasmids are presented in Fig. 4B. As indicated, all three miRNAs significantly downregulated both rs11275300:C and rs11275300:G alleles (in terms of luciferase activity) compared with control miRNA. Notably, the relative luciferase activity was significantly lower in the presence of the major C allele than the minor G allele in cells cotransfected with the hsa-miR-4672 mimic ($P = 0.022$; Fig. 4C), whereas no significant differences were observed in the hsa-miR-6768-5p or hsa-miR-1910-5p group (Fig. 4D and E). These results suggest that the minor G allele could interfere with the binding affinity of hsa-miR-4672 with *DTL* 3′UTR. A875 cells (CC homozygote) were transfected with the hsa-miR-4672 mimic or hsa-miR-4672 inhibitor to further assess the regulatory effect of hsa-miR-4672 on *DTL* in melanoma, and the results showed that hsa-miR-4672 could downregulate *DTL* expression at both mRNA and protein levels by directly targeting the 3′UTR of *DTL* (Fig. 4F and G).

3.7. Associations among the rs11275300 genotype, hsa-miR-4672 and DTL expression in AM

We further confirmed the correlation between *DTL* mRNA and hsa-miR-4672 expression in 48 fresh frozen

primary AM specimens with different genotypes of rs11275300 by qRT-PCR. We divided the cohort into low and high hsa-miR-4672 expression groups, and the median value was chosen as the cut-off point. The expression of *DTL* mRNA and hsa-miR-4672 revealed a significant inverse correlation (Pearson correlation coefficient = −0.816, $P < 0.001$; Fig. 5A). The expression of *DTL* mRNA was significantly decreased in the hsa-miR-4672 high expression group compared with the hsa-miR-4672 low expression group ($P < 0.001$; Fig. 5B), but no significant association between the rs11275300 genotype and miR-4672 expression was observed (Fig. 5C). Furthermore, we observed that *DTL* mRNA expression was significantly higher in patients with the rs11275300:G allele compared with those with the CC genotype ($P = 0.043$; Fig. 5D), which was consistent with the results of the IHC analysis.

4. Discussion

DTL along with cytokine receptor-like 4 (CRL4) forms the $CRL4^{Cdt2}$ ligase complex, which can cause ubiquitination and degradation of several key proteins involved in genome integrity, DNA repair processes and cell cycle progression, such as chromatin licencing and DNA replication factor 1, cyclin-dependent kinase inhibitor 1A and lysine methyltransferase 5A [30,31]. Our results showed that DTL in Chinese AM was much higher than that in benign nevi. The DTL expression difference in AM and CM was compared by analysing three GEO data sets extracted from the Caucasian population, and the results showed that there was no difference between the two subtypes, which need to be further verified in a large Chinese population–based cohort. In this study, we conducted

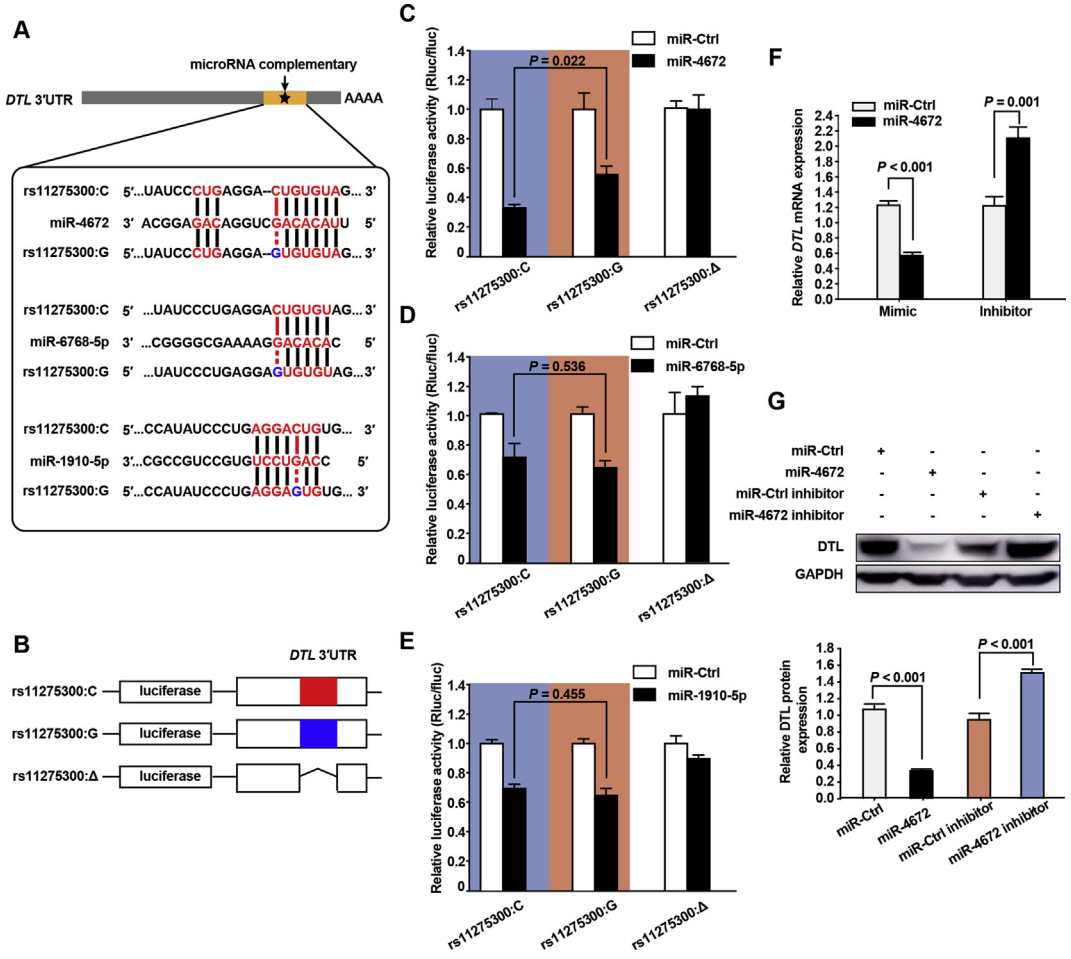

Fig. 4. **Predicted miRNAs that potentially target *DTL* rs11275300**. (A) Predicted miRNA interaction sites within the 3′UTR of *DTL* mRNA including rs11275300. The complementary base pairs are coloured in red, and the position of the rs11275300:G allele is coloured in blue (B) Schema of constructs harbouring different alleles of rs11275300. The 3′UTR of *DTL* was cloned into the SV40 promoter-luciferase–based plasmid. rs11275300:C (red), rs11275300:G (blue), deletion of a putative miRNA site (Δ). (C–E) Luciferase activities were measured after the cotransfection of the reporter constructs with different genotypes of rs11275300 and miRNA mimics or miR-Ctrl in HEK293T cells. Data are presented as mean ± SD of three independent experiments (F, G) A875 cells were transfected with hsa-miR-4672 mimics or inhibitors and the corresponding controls. *DTL* mRNA (F) and protein (G) expression after 48 h of transfection was detected by qRT-PCR and Western blotting. miRNA, microRNA; 3′UTR, 3′-untranslated region; SD, standard deviation; PCR, polymerase chain reaction.

a retrospective exploratory analysis to assess the prognostic value of the tag SNPs of *DTL* in Chinese AM. Two SNPs satisfied the selection criteria, and only rs11275300 was significantly associated with PFS and OS in all cohorts. Furthermore, our results showed that patients with the rs11275300:G allele had a higher plasma LDH level compared with patients with the CC genotype, also indicating that the rs11275300:G allele might be associated with the severity of AM. However, when we detected its clinical significance in patients with non-acral CM, no association between the rs11275300 genotype with survival in CM was observed, which means that the effect of rs11275300 might be specific to the AM subtype. This might be because the genetic background differs between the subtypes as CM has a much higher somatic mutation burden than AM, and other coexisting genetic aberrations might influence DTL expression or biological function. The *in vitro* analysis results suggested that the poor prognosis might be due to allele-specific increase in DTL expression, which was consistent with the observation of higher *DTL* expression causing shorter DFS and OS in CM [16]. As race and ethnicity differences could affect disease susceptibility and response to precision medicine [32,33], whether the prognosis value of rs11275300 can be applied in other ethnicities still needs to be further validated.

DTL is unlikely to function as a classical oncogene because studies have suggested that it might act as a cancer-associated gene to which cancer cells become 'addicted'. The term 'non-oncogene addiction' has been coined particularly to refer to the increased dependence of cancer cells on certain non-oncogenic genes for normal cellular functions [34]. This is supported by a previous finding that DTL depletion can induce apoptosis in different cancer cell lines without affecting non-cancer cell lines [35]. The 'non-oncogene addiction' feature facilitates DTL signalling as a potential therapeutic target. Pevonedistat (MLN4924) is an inhibitor of $CRL4^{Cdt2}$ E3 ubiquitin ligase activator NEDD8-activating enzyme, and Benamar *et al.* [16] proved that $CRL4^{Cdt2}$ inactivation by pevonedistat can induce permanent growth arrest in malignant melanoma cells but not in immortalised melanocytic cell lines. Wong *et al.* [36] also demonstrated the antitumour activity of pevonedistat in melanoma cell lines and patient-derived tumour xenografts. A phase I clinical trial (NCT01011530) has been conducted to assess the safety and antitumour activity of pevonedistat in patients with metastatic melanoma, which has shown that pevonedistat is generally well tolerated in patients with melanoma and that some patients could benefit from pevonedistat treatment [37]. Recently developed novel therapeutic approaches for metastatic melanoma include targeting specific driver mutations and

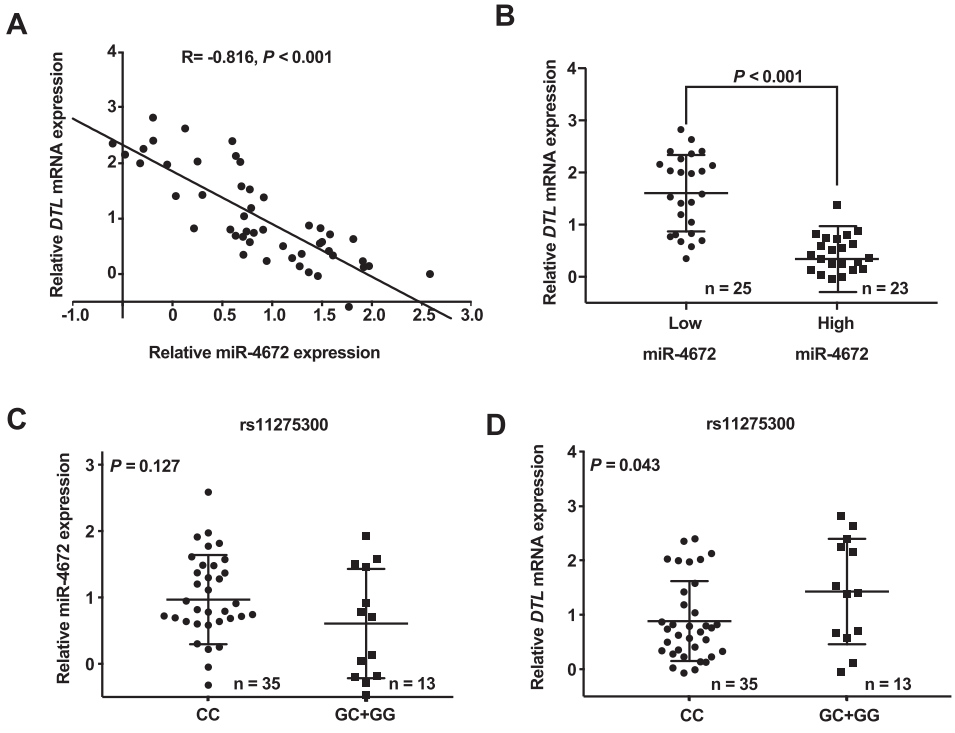

Fig. 5. **The G allele of rs11275300 influences the post-translational modulation of hsa-miR-4672 on *DTL* in AM**. (A, B) *DTL* mRNA levels were inversely correlated with hsa-miR-4672 expression. The *DTL* mRNA and hsa-miR-4672 levels were measured by qRT-PCR and expressed on a $\log_{10}$ scale. High expression of hsa-miR-4672 was considered to be above the optimal cut-off for the median. Correlation between hsa-miR-4672 (C) and *DTL* mRNA (D) expression levels and the rs11275300 genotype. Significance was assessed by the unpaired *t*-test. AM, acral melanoma; PCR, polymerase chain reaction.

checkpoint immunotherapies designed to enhance the antitumour immune response. However, more than 70% of Chinese patients with AM are still incapable of benefiting from targeting inhibitors because of the lack of *BRAF* or *CKIT* mutations. Besides, patients with AM are less susceptible to immune checkpoint inhibitors because of lower programmed death-ligand 1 (PD-L1) expression [38] and tumour-infiltrating lymphocyte numbers [39]. Therefore, high-dose interferon-α2b and chemotherapy remain the primary treatments for Chinese patients with AM. In our study, we found that the rs11275300 genotype was correlated with the mRNA and protein expression level of DTL as patients with the rs11275300:G allele had much higher DTL expression compared with those with the CC genotype. Thus, our results support the hypothesis that pevonedistat might be a particularly promising therapeutic approach for patients with AM with the rs11275300:G allele. However, further research with regard to the susceptibility of patients with different rs11275300 genotypes to pevonedistat is warranted.

Besides specifying mRNA cleavage and repressing gene expression at the post-transcriptional level by binding to the 3′UTR of mRNAs, miRNAs are affected by SNPs residing in the 3′UTR region. SNPs within miRNA-binding sites can decrease or increase target mRNA translation by affecting sequence complementarity between the mRNA transcript and miRNA, and they might be associated with cancer risk and prognosis [40]. To date, no clear functional effect of the rs11275300:C > G polymorphism has been established. In the present study, we predicted that the rs11275300:G allele could impair the binding affinity of hsa-miR-4672 with *DTL* mRNA. Luciferase reporter assay results indicated that the rs11275300:G allele could reduce the suppressive effect of hsa-miR-4672 and cause increased *DTL* expression. Furthermore, we confirmed the inverse correlation between *DTL* and hsa-miR-4672 expression in AM. Altogether, the genotype of rs11275300 in the 3′UTR of *DTL* is involved in the post-transcriptional regulation of DTL protein expression, indicating that rs11275300:G is a gain-of-function variant.

In summary, our research confirms that the rs11275300:G allele in the 3′UTR of *DTL* can be used as an indicator of unfavourable prognosis in patients with AM and provides further evidence that the impairment of the hsa-miR-4672 binding affinity is a relevant pathomechanism. Our findings highlight the close involvement of *DTL* rs11275300:C > G in AM and draw further attention to targeted therapeutic approaches for patients with the rs11275300:G allele.

Conflict of interest statement

None declared.

Acknowledgements

This work was supported by the Beijing Talents Foundation (2016000021223ZK18), the National Natural Science Foundation of China (81672696, 81402264), and Beijing Municipal Administration of Hospitals Clinical Medicine Development of Special Funding Support (ZYLX201603).

Appendix A. Supplementary data

Supplementary data to this article can be found online at https://doi.org/10.1016/j.ejca.2019.06.006.

References

[1] Curtin JA, Fridlyand J, Kageshita T, Patel HN, Busam KJ, Kutzner H, et al. Distinct sets of genetic alterations in melanoma. N Engl J Med 2005;353:2135–47. https://doi.org/10.1056/NEJMoa050092.

[2] Bradford PT, Goldstein AM, McMaster ML, Tucker MA. Acral lentiginous melanoma: incidence and survival patterns in the United States, 1986-2005. Arch Dermatol 2009;145:427–34. https://doi.org/10.1001/archdermatol.2008.609.

[3] Hudson DA, Krige JE. Melanoma in black South Africans. J Am Coll Surg 1995;180:65–71.

[4] Chi Z, Li S, Sheng X, Si L, Cui C, Han M, et al. Clinical presentation, histology, and prognoses of malignant melanoma in ethnic Chinese: a study of 522 consecutive cases. BMC Canc 2011;11:85. https://doi.org/10.1186/1471-2407-11-85.

[5] Roh MR, Kim J, Chung KY. Treatment and outcomes of melanoma in acral location in Korean patients. Yonsei Med J 2010;51:562–8. https://doi.org/10.3349/ymj.2010.51.4.562.

[6] Hayward NK, Wilmott JS, Waddell N, Johansson PA, Field MA, Nones K, et al. Whole-genome landscapes of major melanoma subtypes. Nature 2017;545:175–80. https://doi.org/10.1038/nature22071.

[7] Cancer Genome Atlas N. Genomic classification of cutaneous melanoma. Cell 2015;161:1681–96. https://doi.org/10.1016/j.cell.2015.05.044.

[8] Beadling C, Jacobson-Dunlop E, Hodi FS, Le C, Warrick A, Patterson J, et al. KIT gene mutations and copy number in melanoma subtypes. Clin Cancer Res : An Off J Am Assoc Cancer Res 2008;14:6821–8. https://doi.org/10.1158/1078-0432.ccr-08-0575.

[9] Si L, Kong Y, Xu X, Flaherty KT, Sheng X, Cui C, et al. Prevalence of BRAF V600E mutation in Chinese melanoma patients: large scale analysis of BRAF and NRAS mutations in a 432-case cohort. Eur J Cancer 2012;48:94–100. https://doi.org/10.1016/j.ejca.2011.06.056.

[10] Pan HW, Chou HY, Liu SH, Peng SY, Liu CL, Hsu HC. Role of L2DTL, cell cycle-regulated nuclear and centrosome protein, in aggressive hepatocellular carcinoma. Cell Cycle 2006;5:2676–87. https://doi.org/10.4161/cc.5.22.3500.

[11] Mackintosh C, Ordonez JL, Garcia-Dominguez DJ, Sevillano V, Llombart-Bosch A, Szuhai K, et al. 1q gain and CDT2 overexpression underlie an aggressive and highly proliferative form of Ewing sarcoma. Oncogene 2012;31:1287–98. https://doi.org/10.1038/onc.2011.317.

[12] Pan WW, Zhou JJ, Yu C, Xu Y, Guo LJ, Zhang HY, et al. Ubiquitin E3 ligase CRL4(CDT2/DCAF2) as a potential chemotherapeutic target for ovarian surface epithelial cancer. J Biol Chem 2013;288:29680–91. https://doi.org/10.1074/jbc.M113.495069.

[13] Ueki T, Nishidate T, Park JH, Lin ML, Shimo A, Hirata K, et al. Involvement of elevated expression of multiple cell-cycle regulator, DTL/RAMP (denticleless/RA-regulated nuclear matrix associated protein), in the growth of breast cancer cells. Oncogene 2008;27:5672–83. https://doi.org/10.1038/onc.2008.186.
[14] Kobayashi H, Komatsu S, Ichikawa D, Kawaguchi T, Hirajima S, Miyamae M, et al. Overexpression of denticleless E3 ubiquitin protein ligase homolog (DTL) is related to poor outcome in gastric carcinoma. Oncotarget 2015;6:36615–24. https://doi.org/10.18632/oncotarget.5620.
[15] Talantov D, Mazumder A, Yu JX, Briggs T, Jiang Y, Backus J, et al. Novel genes associated with malignant melanoma but not benign melanocytic lesions. Clin Cancer Res : An Off J Am Assoc Cancer Res 2005;11:7234–42. https://doi.org/10.1158/1078-0432.Ccr-05-0683.
[16] Benamar M, Guessous F, Du K, Corbett P, Obeid J, Gioeli D, et al. Inactivation of the CRL4-CDT2-SET8/p21 ubiquitylation and degradation axis underlies the therapeutic efficacy of pevonedistat in melanoma. EBioMedicine 2016;10:85–100. https://doi.org/10.1016/j.ebiom.2016.06.023.
[17] Conne B, Stutz A, Vassalli JD. The 3' untranslated region of messenger RNA: a molecular 'hotspot' for pathology? Nat Med 2000;6:637–41. https://doi.org/10.1038/76211.
[18] Mignone F, Gissi C, Liuni S, Pesole G. Untranslated regions of mRNAs. Genome Biol 2002;3. REVIEWS0004.
[19] Bartel DP. MicroRNAs: genomics, biogenesis, mechanism, and function. Cell 2004;116:281–97.
[20] Sethupathy P, Collins FS. MicroRNA target site polymorphisms and human disease. Trends Genet : TIG (Trends Genet) 2008;24:489–97. https://doi.org/10.1016/j.tig.2008.07.004.
[21] Liu S, Tetzlaff MT, Liu A, Liegl-Atzwanger B, Guo J, Xu X. Loss of microRNA-205 expression is associated with melanoma progression. Lab Investig 2012;92:1084–96. https://doi.org/10.1038/labinvest.2012.62.
[22] Yu Z, Li Z, Jolicoeur N, Zhang L, Fortin Y, Wang E, et al. Aberrant allele frequencies of the SNPs located in microRNA target sites are potentially associated with human cancers. Nucleic Acids Res 2007;35:4535–41. https://doi.org/10.1093/nar/gkm480.
[23] Brewster BL, Rossiello F, French JD, Edwards SL, Wong M, Wronski A, et al. Identification of fifteen novel germline variants in the BRCA1 3'UTR reveals a variant in a breast cancer case that introduces a functional miR-103 target site. Hum Mutat 2012;33:1665–75. https://doi.org/10.1002/humu.22159.
[24] Xu T, Ma M, Dai J, Yu S, Wu X, Tang H, et al. Gene expression screening identifies CDCA5 as a potential therapeutic target in acral melanoma. Hum Pathol 2018;75:137–45. https://doi.org/10.1016/j.humpath.2018.02.009.
[25] Liu C, Zhang F, Li T, Lu M, Wang L, Yue W, et al. MirSNP, a database of polymorphisms altering miRNA target sites, identifies miRNA-related SNPs in GWAS SNPs and eQTLs. BMC Genomics 2012;13:661. https://doi.org/10.1186/1471-2164-13-661.
[26] Agarwal V, Bell GW, Nam JW, Bartel DP. Predicting effective microRNA target sites in mammalian mRNAs. Elife 2015;4. https://doi.org/10.7554/eLife.05005.
[27] Kozomara A, Griffiths-Jones S. miRBase: annotating high confidence microRNAs using deep sequencing data. Nucleic Acids Res 2014;42:D68–73. https://doi.org/10.1093/nar/gkt1181.
[28] Bhattacharya A, Ziebarth JD, Cui Y. PolymiRTS Database 3.0: linking polymorphisms in microRNAs and their target sites with human diseases and biological pathways. Nucleic Acids Res 2014;42:D86–91. https://doi.org/10.1093/nar/gkt1028.
[29] Rehmsmeier M, Steffen P, Hochsmann M, Giegerich R. Fast and effective prediction of microRNA/target duplexes. RNA 2004;10:1507–17. https://doi.org/10.1261/rna.5248604.
[30] Sansam CL, Shepard JL, Lai K, Ianari A, Danielian PS, Amsterdam A, et al. DTL/CDT2 is essential for both CDT1 regulation and the early G2/M checkpoint. Genes Dev 2006;20:3117–29. https://doi.org/10.1101/gad.1482106.
[31] Abbas T, Dutta A. CRL4Cdt2: master coordinator of cell cycle progression and genome stability. Cell Cycle 2011;10:241–9. https://doi.org/10.4161/cc.10.2.14530.
[32] Ferlay J, Soerjomataram I, Dikshit R, Eser S, Mathers C, Rebelo M, et al. Cancer incidence and mortality worldwide: sources, methods and major patterns in GLOBOCAN 2012. Int J Cancer 2015;136:E359–86.
[33] Cormier JN, Xing Y, Ding M, Lee JE, Mansfield PF, Gershenwald JE, et al. Ethnic differences among patients with cutaneous melanoma. Arch Intern Med 2006;166:1907–14. https://doi.org/10.1001/archinte.166.17.1907.
[34] Luo J, Solimini NL, Elledge SJ. Principles of cancer therapy: oncogene and non-oncogene addiction. Cell 2009;136:823–37. https://doi.org/10.1016/j.cell.2009.02.024.
[35] Olivero M, Dettori D, Arena S, Zecchin D, Lantelme E, Di Renzo MF. The stress phenotype makes cancer cells addicted to CDT2, a substrate receptor of the CRL4 ubiquitin ligase. Oncotarget 2014;5:5992–6002. https://doi.org/10.18632/oncotarget.2042.
[36] Wong KM, Micel LN, Selby HM, Tan AC, Pitts TM, Bagby SM, et al. Targeting the protein ubiquitination machinery in melanoma by the NEDD8-activating enzyme inhibitor pevonedistat (MLN4924). Investig New Drugs 2017;35:11–25. https://doi.org/10.1007/s10637-016-0398-8.
[37] Bhatia S, Pavlick AC, Boasberg P, Thompson JA, Mulligan G, Pickard MD, et al. A phase I study of the investigational NEDD8-activating enzyme inhibitor pevonedistat (TAK-924/MLN4924) in patients with metastatic melanoma. Investig New Drugs 2016;34:439–49. https://doi.org/10.1007/s10637-016-0348-5.
[38] Kaunitz GJ, Cottrell TR, Lilo M, Muthappan V, Esandrio J, Berry S, et al. Melanoma subtypes demonstrate distinct PD-L1 expression profiles. Lab Investig 2017;97:1063–71. https://doi.org/10.1038/labinvest.2017.64.
[39] Castaneda CA, Torres-Cabala C, Castillo M, Villegas V, Casavilca S, Cano L, et al. Tumor infiltrating lymphocytes in acral lentiginous melanoma: a study of a large cohort of cases from Latin America. Clin Transl Oncol 2017;19:1478–88. https://doi.org/10.1007/s12094-017-1685-3.
[40] Liu Y, Xu J, Jiang M, Ni L, Chen Y, Ling Y. Association between functional PSMD10 Rs111638916 variant regulated by MiR-505 and gastric cancer risk in a Chinese population. Cell Physiol Biochem : Int J Exp Cell Physiol, Biochem, Pharmacol 2015;37:1010–7. https://doi.org/10.1159/000430227.